APPENDIX B

ADDITIONAL MATERIAL FOR COSMIC RAY REJECTION

In this appendix we provide additional supporting material to help further explain the selection criteria used to reduce cosmic ray backgrounds which are the dominant background in this analysis. As described in Chapter 4, cosmic rays produce photons in the detector. As shown in Figure 4.1, cosmic rays are, in general, particles that originate in outer space and then interact with the Earth's atmosphere producing secondary particles that then shower down to the Earth's surface. The majority of particles that interact with our detector are muons as they have a long enough lifetime and small enough cross section with ordinary matter to reach the detector. If a cosmic ray happens to deposit energy in the detector, in particular the EM calorimeter, it can mimic a photon candidate signature (i.e., an energy deposit in the EM calorimeter only and no track pointing to it in from the tracking chamber). If this deposit occurs in coincidence with a collision in the detector it can lead to both an incorrectly assigned photon to a vertex that had nothing to do with its production as well as leaving an imbalance of energy in the detector which is misidentified as $\not{E}_T$. This mis-identification of a photon can occur if the cosmic ray produces an electromagnetic cluster via the the emission of a real, high-energy photon inside the detector that occurs as the cosmic ray traverses the detector or if the cosmic ray undergoes a bremsstrahlung interaction or a high q^2 interaction within the EM calorimeter. While only a small fraction of cosmic ray collisions fake the photon signature, the sheer flux of cosmic rays makes them a significant background in our search.

There are a number of features which allow us to separate photons from cosmic ray sources from physics sources. While many standard techniques have been created over the years [76], what makes this task particularly difficult in this analysis is that we are trying to identify photons emanated from a new particle that traveled for awhile before decaying to a photon (see Figure 1.7). Thus, the photon can hit the calorimeter face at an incident angle that is different from photons that come from the beam line. Unfortunately, many of the vetos for cosmic rays were developed based on just this difference requiring that the photon comes directly from the beam line. For example, the CES χ^2 selection requirement in the standard photon identification requirement. Luckily there are many other features which allow us to develop a series of cuts to help veto against mis-identifying an photon candidate from a cosmic ray event. We next describe three sets of requirements designed to remove events in our sample from cosmic ray sources.

Before we begin it is worth saying how we will estimate the rejection power and efficiency of these requirements. Since we have large number of cosmic rays in our data, we select a pure sample of cosmics using γ+$\not\!\!E_T$ data, using the sample of events that pass all the requirements in Table 4.1, but requiring 20 ns $< t_{corr} <$ 80 ns to create a pure sample cosmics. Other cuts will be added as is useful/necessary. For our efficiency measurements we a clean sample of W$\rightarrow e\nu \rightarrow e + \not\!\!E_T$ events. Recall, as discussed in Section 2.4.5, electrons do a good job of simulating photons in the calorimeter, but provide a pure sample of collision events.

B.1 Muon Stub Cosmic Ray Rejection

We begin by describing a veto used to reject photon events coming from cosmic rays that is based on the presence of activity in the muon chambers just outside the location of the photon candidate in the calorimeter. This method has been used at CDF and in previous delayed photon searches with great success [38, 76]. The veto focuses on cosmic ray that have traversed the muon chambers as it entered the detector and then deposited a significant amount of energy in a nearby EM calorimeter tower creating a photon candidate. Our rejection technique is designed to find this topology.

Since our search strategy starts by focusing on the using of the 'outside-in' topology of the majority cosmic ray events, we look to the muon detector, which is on the outside radius of the CDF detector, for activity which corresponds to the electromagnetic shower we see in the calorimeter. As described in Chapter 2, the muon system is a series of 4 layer single wire proportional drift chamber. A schematic of the CDF detector with the muon systems highlighted is shown in Figure B.1. When a muon passes through this system it creates a series of "hits" along the trajectory regardless of whether it comes from the outside in, or from the inside out. In the typical muon identification procedure, an algorithm searches for sets of hits which could be from the presence of such a muon trajectory in the muon chambers. If it finds a grouping of such hits its position is determined and the collection is labeled a "stub". After this, a second algorithm then searches for tracks in the COT that point to this outer "stub". For collision-based muons, if there is a track pointing to a muon-stub this combination is identified as a collision muon. A cosmic ray will often leave a muon stub, but no track in the COT (the trajectory would be moving backwards in time and so would not be reconstructed). It is these types of stubs that we search for (i.e. stubs without an associated track) which lie within a close angle to the photon candidate. The final requirement is that if we find a muon stub within a $|\Delta\phi| <30$ degrees we veto that event as likely having come from a cosmic ray.

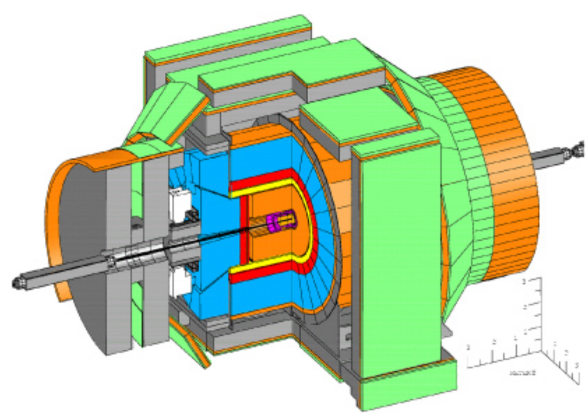

Fig. B.1. Schematic view of the CDF detector where the muon detection system is highlighted in green. These muon detectors allow us to distinguish cosmic rays which originate outside the detector and pass through the muon detectors and may be incorrectly identified as a photon.

Using our pure cosmic ray sample the muon-stub veto is found to reject >85% of cosmic ray candidates while being >95% efficient for electron data [76]. The inefficiency comes from cosmics which produce a stub that occur in coincidence with the event but do not produce a photon. This veto has been used as a standard CDF cosmic veto for many years and we utilize this veto "as is" without any additional optimization.

B.2 Hadronic Energy Fraction Selection Criteria for Cosmics Rays

A second requirement considers the amount of energy deposited in the hadronic calorimeter to separate cosmic ray sources from photons that come from collisions. We expect high energy photons from collisions to end up showering mostly in the EM calorimeter but leaves some small fraction of their energy in the HAD calorimeter. In addition, we expect the amount of energy deposited in the HAD to scale with the total photon energy. However, cosmic ray photons resulting from bremsstrahlung interactions or a high q^2 collision in the EM calorimeter will leave very little energy in the hadronic calorimeter on average.

To compare the deposition of energy in the calorimeter we consider our same sample of cosmics and electrons but also require a muon stub within a $|\Delta\phi| < 30°$ help us focus on cosmics that are not already rejected. The hadronic energy distribution can be seen in Figure B.2 where we have scaled the amount of energy deposted in the HAD in conjunction with the total energy deposited. Specifically, you can see a great deal more hadronic energy is deposited by high energy electrons then cosmic ray photons. To separate photons from collision sources from photons candidates from cosmics we required each candidate to pass HAD(E) $\geq -0.30 + 0.008 \cdot E_T$. We find this cut to be 95% efficicient and reject ∼66% of cosmic candidate events.

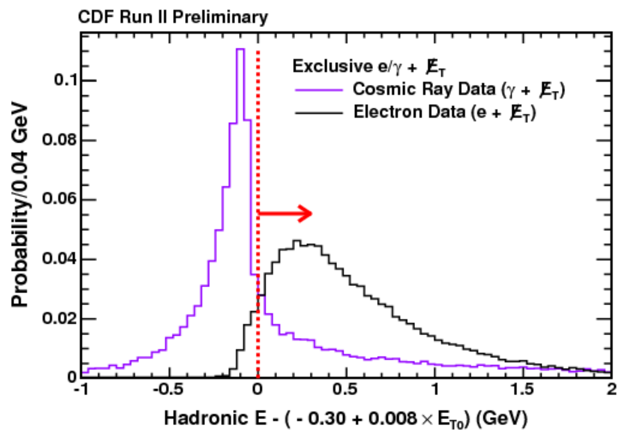

Fig. B.2. The distribution of the modified version of HAD(E), taking into account the photon candidate energy, for electrons coming from collisions using selection requirements in Table 3.1 (black line) as well as the hadronic energy distribution coming from cosmic ray photons using the selection requirements in Table 4.1 (pink line) and reversing the muon-stub veto in Table 4.2. We note that high energy objects coming from the collision deposit more energy in the hadronic calorimeter then minimum ionizing events like cosmic rays. The dashed line shows our requirement.

B.3 Central Electromagnetic Shower Energy Selection Criteria for Cosmics Rays

An additional requirement to help reject cosmic ray backgrounds takes advantage of the fact that cosmic rays photons often interact with the EM calorimeter by a single high q^2 interaction in the detector. This produces a lot of light in just a few layers of the calorimeter rather than the deposition being consistent with a full shower coming from the beam line. Thus, the amount of energy deposited near shower maximum (and measured by the CES) is typically small. By way of contrast a photon that hits the calorimeter and fully showers will have its shower maximum at the CES and deposits a lot of energy there. Since a coarse measurement of the total energy can be determined using the CES alone (CES(E)), we compare its measurement to the measurement from the full tower.

Since the energy deposition in the CES is very different for cosmics and real photons we use this to reject cosmic ray sources. To do this we have two cuts, one on the total energy deposited in the CES, CES(E)>10 GeV, as well as one that considers the fraction of CES energy over the total energy to help distinguish from high energy collision photons and photons coming from cosmic rays ($\frac{\mathrm{CES(E)}}{\mathrm{TotalE}}$). Figure B.3 shows the ratio for identified cosmic rays versus electrons coming from a collision is shown in Figure B.3 and using the same samples as in the previous section, but after the HAD requirements as well.

The combination of all three cosmic ray rejection requirements are very powerful. As shown in Figure B.4, when we make a cut $\frac{\mathrm{CES(E)}}{\mathrm{TotalE}} > 0.2$ in addition to the Hadronic Energy sliding cut we have an overall 92% efficiency for a 76% rejection of cosmic ray photons.

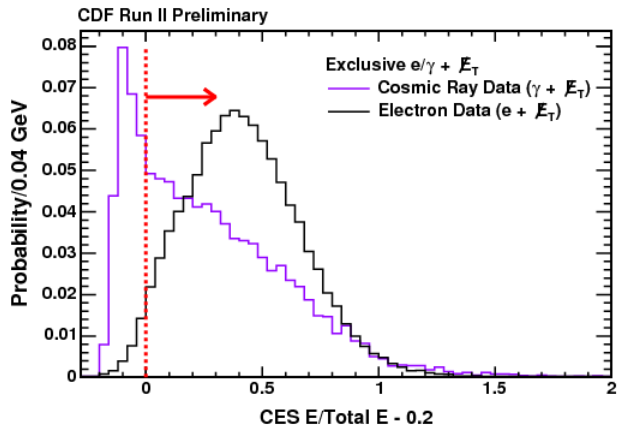

Fig. B.3. This plot shows a comparison of $\frac{\text{CES(E)}}{\text{TotalE}}$ for cosmic ray photons identified (pink line) using the selection requirements in Tables 4.1 and 4.2 and (black line) electrons using Table 3.1. We note that high energy objects coming from the collision deposit a larger fraction of their energy in the CES detector then photon candidates from cosmic ray sources do.

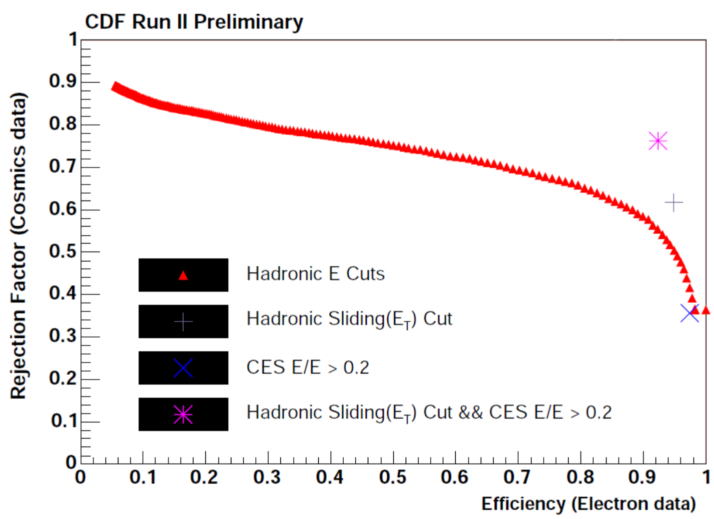

Fig. B.4. Rejection versus efficiency curve for the combination of the Had(E) cut and the CES energy fraction taken together resulting in a 92% efficency for a 76% rejection of cosmic ray photons.